

Mechanoactive Scaffold Induces Tendon Remodeling and Expression of Fibrocartilage Markers

Jeffrey P. Spalazzi MS, Moira C. Vyner,
Matthew T. Jacobs MS, Kristen L. Moffat MS,
Helen H. Lu PhD

Published online: 30 May 2008
© The Association of Bone and Joint Surgeons 2008

Abstract Biological fixation of soft tissue-based grafts cellularity, proteoglycan content, and gene expression over for anterior cruciate ligament (ACL) reconstruction poses a 2-week period. Scaffold contraction resulted in over 15% major clinical challenge. The ACL integrates with sub-compression of the patellar tendon graft and upregulated chondral bone through a fibrocartilage enthesis, which the expression of fibrocartilage-related markers such as serves to minimize stress concentrations and enables load transfer between two distinct tissue types. Functional factor- β 3 (TGF- β 3). Additionally, proteoglycan content integration thus requires the reestablishment of this was higher in the compressed tendon group after 1 day. Fibrocartilage interface on reconstructed ACL grafts. The data suggest the potential of a mechanoactive scaffold designed and characterized a novel mechanoactive scaffold promote the formation of an anatomic fibrocartilage based on a composite of polyhydroxyester nanofibers enthesis on tendon-based ACL reconstruction grafts. and sintered microspheres; we then used the scaffold to test the hypothesis that scaffold-induced compression of tendon grafts would result in matrix remodeling and the expression of fibrocartilage interface-related markers. Histology coupled with confocal microscopy and biochemical assays were used to evaluate the effects of scaffold-induced compression on tendon matrix collagen distribution.

Each author certifies that he or she has no commercial associations (eg, consultancies, stock ownership, equity interest, patent/licensing arrangements, etc) that might pose a conflict of interest in connection with the submitted article. This study was funded by a research award from the Musculoskeletal Transplant Foundation. Each author certifies that his or her institution has approved the animal protocol for this investigation and that all investigations were conducted in conformity with ethical principles of research.

J. P. Spalazzi, M. C. Vyner, M. T. Jacobs,
K. L. Moffat, H. H. Lu (✉)
Department of Biomedical Engineering, Biomaterials and
Interface Tissue Engineering Laboratory, Columbia University,
351 Engineering Terrace Building, MC 8904, 1210 Amsterdam
Avenue, New York, NY 10027, USA
e-mail: hl2052@columbia.edu

H. H. Lu
College of Dental Medicine, Columbia University, New York,
NY, USA

Introduction
The anterior cruciate ligament (ACL) is the most frequently injured ligament of the knee [1], with over 300,000 injuries reported [2] and more than 100,000 ACL reconstruction procedures performed annually in the United States. Primary ACL reconstruction has traditionally utilized autologous bone-patellar tendon-bone (BPTB) grafts, with a shift in recent years toward the semitendinosus or hamstring tendon grafts [3, 4] due to patellar tendonitis and anterior knee pain related to BPTB grafts. Allografts are also used for ACL reconstruction [5, 6], with the tibialis and Achilles tendons being the most common [7, 8, 9, 10, 11, 12]. The long-term performance of ACL grafts depends on several factors, including the structural and material properties of the graft, the initial graft tension [13, 14, 15, 16, 17], the intraarticular position of the graft [18, 19], and graft fixation [20, 21]. Increased emphasis has been placed on graft fixation since postsurgical rehabilitation regimens require the immediate ability to regain the full range of motion, reestablish neuromuscular function, and bear weight [22, 23]. The BPTB graft has been the gold standard for ACL reconstruction in part

due to its ability to integrate with subchondral bone via the compressive loading led to a decrease in the size of the bony ends. Moreover, it possesses intact insertion sites on the articular surface, breakdown of the collagen fiber network, and lower matrix glycosaminoglycan content soft tissue and bone. In contrast, the autologous hamstring tendon graft and tendon allografts must be fixed mechanically within the femoral bone tunnel via a transfemoral and interference screw, while an interference screw with a washer or staple is used to fix the graft within the tibial tunnel. Although the physiological range of motion may be possible via mechanical fixation, graft-to-bone integration is not achieved as the native insertion site is lost during surgery, with nonmineralized soft tissue found within the bone tunnels [9, 33, 54]. Thus graft fixation at the tibial and femoral tunnels, instead of the isolated strength of the graft, represents the weakest points during the early postoperative healing period [33, 53, 55].

To address the challenge of achieving biological fixation of soft tissue-based ACL reconstruction grafts, our goal was to develop functional methods to regenerate an anatomic transition on these grafts. To this end, the potential of two types of mechanoactive scaffold systems that can directly apply compressive mechanical loading to soft tissue grafts were evaluated. Specifically, the first scaffold system consisted of an aligned poly(lactide-co-glycolic acid) (PLGA) nanofiber mesh [66], while the second system combined the aligned mesh with a degradable scaffold [8, 60] fabricated from PLGA.

Our first objective was to characterize the contractile properties of the nanofiber mesh as well as the biphasic contraction of the nanofiber meshes [30]. Our second objective was to evaluate the effect of scaffold-induced compression on matrix remodeling and the development of proteoglycan-related markers. We hypothesized that with the inherent contractile properties of the nanofiber mesh, compressive mechanical loading would be applied to tendon grafts by the mechanoactive scaffold, resulting in matrix remodeling and leading to proteoglycan formation.

The ACL inserts into subchondral bone through an articular interface, which serves to minimize the formation of stress concentrations and facilitates load transfer between two distinct tissue types [3, 44, 46, 61, 67, 68].

While the mechanism governing interface formation is not well understood, metaplasia of tendon or ligament has been reported to play a role [8]. Using a rodent model, Nawata et al. [47] reported that during development, ACL insertion percentage change in length ($n=5$) and width ($n=5$) of fibrochondrocytes are derived from ligament fibroblasts [4].

To determine the effects of scaffold design on the resultant contraction exerted by each scaffold system, we measured the nanofiber mesh as well as scaffold diameter (3) as a function of scaffold design (mesh versus mesh-collar). Mechanical stimulation is reportedly important for fibroblast differentiation into fibrochondrocytes and subsequent proteoglycan formation [4]. Vogel et al. [32, 41, 48, 52] on proteoglycan development on a tendon graft we determined the effect of scaffold-induced compression on proteoglycan formation in flexor tendons. It was reported that compression induced metaplasia of tendinous matrix and initiated transformation into proteoglycan. For example, while gene expression for proteoglycan-related markers such as Type II collagen ($n=2$), aggrecan ($n=2$), and transforming growth factor- β ($n=2$) were determined using reverse-transcription polymerase chain reaction (RT-PCR). All above parameters were evaluated as a function of study variables such as scaffold-induced compression (with versus without compression) and culdiorum profundus tendon in order to remove turing time (Day 1 versus Day 14).

We obtained bovine patellar tendons from tibiofemoral bioactive glass (BG, 20 μ m; MO-SCI Corporation, Rolla, MO) joints (187 days old, Green Village Packing, Green Village, NJ). Briefly, the joints were first cleaned in an antiseptic bath (20 wt% to a solution of PLGA and dichloroantimicrobial bath). Under antiseptic conditions, midline methane (Acros Organics, Morris Plains, NJ). After longitudinal incisions were made through the subcutaneous cortex, the suspension was poured into a 1% solution of fascia to expose the patellar tendon. The paratenon was removed, and the patellar tendon dissected from the underlying fat pad. Sharp incisions were made through the patellar tendon at the patellar and tibial ends in order to remove the insertions from the graft.

For scaffold fabrication, the aligned nanofiber meshes (Fig. 1A) were formed by electrospinning a viscous polymer solution consisting of 35% poly(D,L-lactide-co-glycolic acid) or PLGA 85:15 (I.V.= 0.70 dL/g, Lakeshore Biomaterials, Birmingham, AL), 55% N,N-dimethylformamide (Sigma, St. Louis, MO), and 10% fetal bovine serum (FBS, Atlanta Biologicals, Norcross, GA) and incubated at 37°C and 5% CO₂. The meshes were loaded into a syringe fitted with an 18-gauge needle (Becton Dickinson, Franklin Lakes, NJ). Aligned fibers were obtained using an aluminum drum rotating at a velocity of 20 m/s. A constant flow rate of 1 mL/hr was maintained using a syringe pump (Harvard Apparatus, Holliston, MA), and an electrical potential was applied

between the needle and the grounded substrate (distance = 10 cm) using a high-voltage DC power supply mediated compression of the microsphere-based graft collar (Spellman, Hauppauge, NY). For scaffold characterization, fiber morphology, diameter, and alignment of the as-fabricated mesh samples were analyzed using scanning electron microscopy (SEM, JSM 5600LV, JEOL, Tokyo, Japan). Briefly, the samples were sputter-coated with gold (LVC-76, Plasma Sciences, Lorton, VA) and subsequently imaged at a voltage of 5 kV.

To fabricate the tendon graft collar, a scaffold based on sintered microspheres was formed following published methods [38, 60]. Specifically, the scaffold was composed of composite microspheres consisting of PLGA (85:15, I.V. = 3.42 dl/g, Purac, Lincolnshire, IL) and 45S5 cut into 10 cm \times 2 cm strips, with fiber alignment oriented

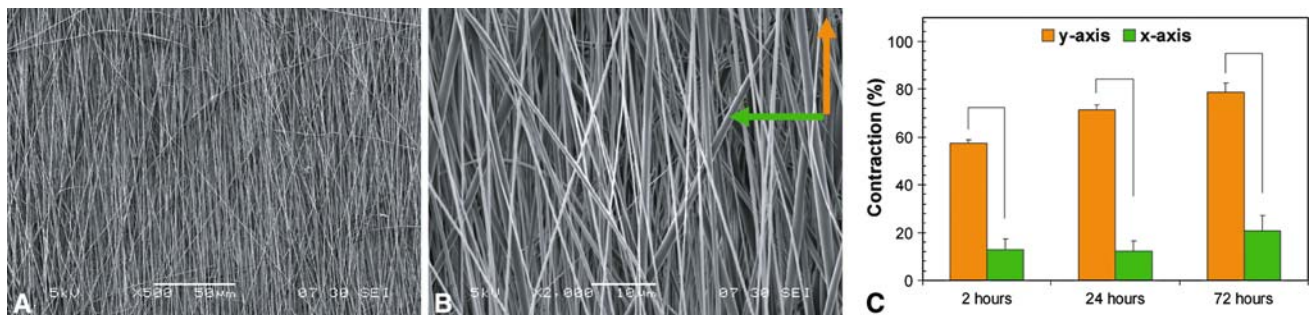


Fig. 1A–C Characterization of nanofiber mesh contraction revealed along the direction of fiber alignment (y-axis) and contraction highly oriented fibers and anisotropic contractile behavior. The as-fabricated nanofiber mesh exhibited a preferential fiber alignment along the y-axis (A) ($p = 2.102 \times 10^{-13}$), 24 hours (B) ($p = 6.719 \times 10^{-15}$), and 72 hours (C) ($p = 1.035 \times 10^{-13}$). (C) Percent contraction of the aligned nanofiber mesh was greatest

along the long axis of the mesh. The patellar tendon graft (DMMB) dye-binding assay [14]. Tissue digest from the was bisected along its long axis, and one-half of the tendon cell quantitation assay was combined with DMMB dye, was wrapped with the nanofiber mesh while the other half and concentration of the GAG-DMMB complexes was served as the unloaded control. The samples were cultured and determined using a plate reader at 540 and 595 nm and in DMEM supplemented with 1% nonessential amino acids, 1% antibiotics, and 0.1% antifungal (all from Mediatech), and 10% FBS (Atlanta Biologicals).

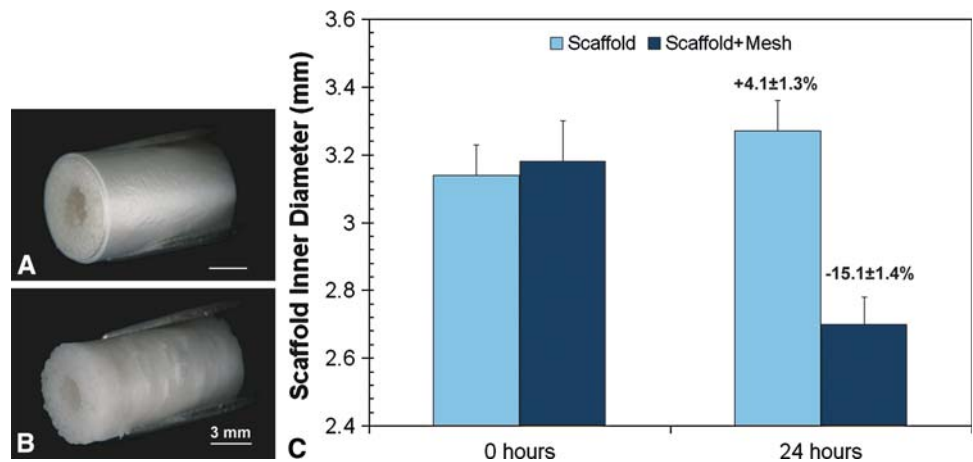
At days 5 and 14, the effects of compression on tissue morphology and cellularity were characterized by histology. The $\beta 3$ (TGF- $\beta 3$) were determined at Day 0 and Day 1 by RT-PCR. Briefly, after removing the graft collar and nanofiber buffered formalin (Fisher Scientific, Pittsburgh, PA), and mesh, we isolated total RNA of the tendon graft using the Trizol extraction method (Invitrogen, Carlsbad, CA). The samples were then cut into 7 μ m thick sections and stained with hematoxylin and eosin (H&E).

The potential of the mesh collar scaffold complex to apply compression to the tendon graft was also evaluated in vitro. Specifically, the patellar tendon graft was dissected into 2 cm \times 0.3 cm segments and the cylindrical scaffold was halved along its long axis. Each tendon segment was inserted between the two scaffold halves. For the experimental group, the tendon graft collar was wrapped with the aligned nanofiber mesh (15.5 \times 1.5 cm), while the control scaffolds were wrapped with precontracted electrospun mesh. In addition, to extend compression of the tendon graft, the experimental group was wrapped with new mesh strips on every other day during the 2-week study period. The complex of mesh collar and tendon graft was cultured in supplemented media at 37°C and 5% CO₂.

We determined the effects of scaffold-induced compression on tendon matrix organization (collagen distribution) at 1 and 14 days using hematoxylin and eosin stains (H&E). Collagen distribution (n = 2) was visualized using Picrosirius red, and organization of the collagen fibers was examined under polarized light microscopy [51, 65]. In addition, since most of the mesh compression occurs within the first 24 hours, total cell number and proteoglycan content (n = 5) in the tendon graft were evaluated at Day 1. For the biochemical assays [26, 27, 60], both the wet and dry weights of the tendon samples were measured at Day 0 and Day 1, and the tissue was subsequently digested for 16 hours in 2% papain (Sigma) buffer at 60°C. We determined total DNA content of the digest with the PicoGreen dsDNA assay (Molecular Probes) following the manufacturer's suggested protocol. Sample fluorescence was measured by a microplate reader (Tecan) with excitation and emission wavelengths set at 485 and 535 nm, respectively. The total DNA content was calculated using the conversion factor of 8 pg DNA/cell [40].

We quantified total sulfated glycosaminoglycan (GAG) content (n = 5) in the compressed and control tendon samples using a colorimetric 1,9-dimethylmethylene blue assay [40]. For the nanofiber mesh-only design, we observed a high degree of alignment with an average fiber diameter of $0.9 \pm 0.4 \mu\text{m}$ (Fig. 1B). Moreover, anisotropic mesh contraction behavior was observed, with higher contraction along the direction of nanofiber alignment at 2 hours (p = 2.102×10^{-12}), 24 hours (p = 6.719×10^{-15}), and 72 hours (p = 1.035×10^{-13}). Specifically, the mesh contracted over 57% along the aligned fiber direction (y-axis) by 2 hours, with less than 13% reduction in the x-axis (Fig. 1C). Mesh contraction continued over time, exhibiting over 70% contraction in the y-axis and 20% in the x-axis by 24 hours and stabilizing thereafter, with no differences between the 24- and 72-hour groups. For the scaffold design with mesh wrapped around a

Fig. 2A–C NanoPber mesh contraction resulted in compression of the graft collar scaffold. A) The microsphere-based graft collar scaffold is wrapped with nanoPber mesh, and B) after 24 hours of mesh contraction. (C) Scaffold inner diameter was reduced due to compression induced by the nanoPber mesh. While the scaffold-only control swelled (4%, $p = 0.146$), nanoPber mesh contraction induced over 15% decrease in scaffold inner diameter after 24 hours ($p = 3.63 \times 10^{-4}$).



microsphere-based graft collar (Fig. 2A), mesh contraction decreased ($p = 3.63 \times 10^{-4}$) scaffold inner diameter, averaging 15% strain within 24 hours (Fig. 2B). In contrast, the control scaffold without mesh expanded and increased in inner diameter (4%, $p = 0.146$) when cultured under similar conditions (Fig. 2C).

Contraction of the aligned nanoPber mesh resulted in an approximately 30% decrease in tendon graft diameter by 24 hours (Fig. 3A, B). After 5 days of explant culture, the compressed tendon exhibited less crimp structure compared to that in the control group and remodeled into a dense matrix with high cellularity (Fig. 3C, D). However, by Day 14, the crimp pattern was restored in the compressed group, with ultrastructure and cellularity loading was maintained over time (Fig. 3E, F).

indistinguishable from the unloaded control group (Fig. 3E, F). When the nanoPber mesh scaffold was used to compress the tendon graft (Fig. 3A, B), contraction of the biphasic scaffold resulted in distinct tendon-graft matrix organization from that of the unloaded control, with an apparent increase in matrix density. The characteristic crimp, with evident disruption of the matrix organization from that of the unloaded control, was less evident in the experimental group (Fig. 3C, D). In contrast, in the tendon graft compressed by the mesh+collar scaffold complex, the matrix remodeling observed at 24 hours following the onset of loading was maintained over time (Fig. 3E, F).

After 24 hours (Fig. 3A, B). After 5 days of explant culture, the compressed tendon exhibited less crimp structure compared to that in the control group and remodeled into a dense matrix with high cellularity (Fig. 3C, D). However, by the mesh+collar scaffold complex, the matrix remodeling observed at 24 hours following the onset of loading was maintained over time (Fig. 3E, F).

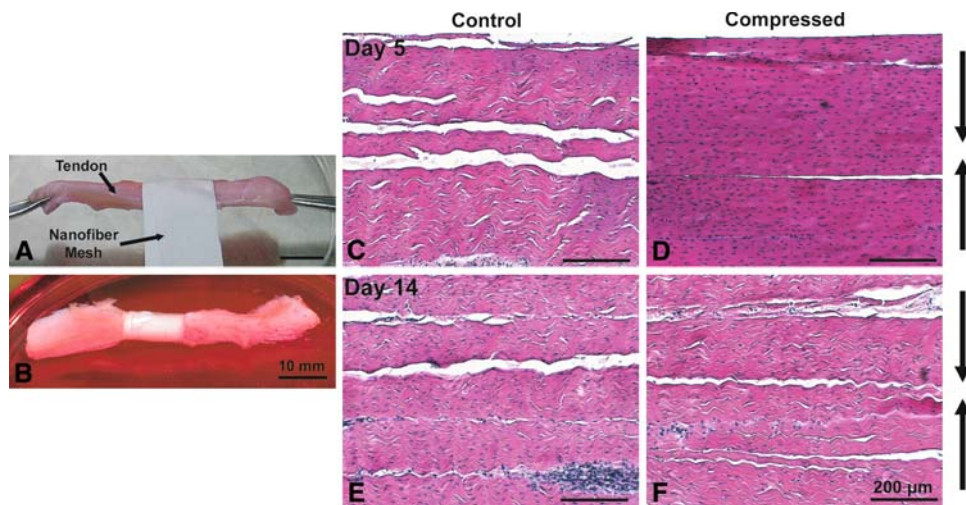


Fig. 3A–F Tendon grafts were compressed radially with the nano-compressed tendon matrix exhibited greater cell density and was morphologically distinct from the unloaded control. After 14 days patellar tendon sample, and B) the samples after 24 hours of mesh contraction. Mesh contraction resulted in tendon matrix organization (F) loaded. (Stain, hematoxylin and eosin; original magnification, $\times 10$). Moreover, the

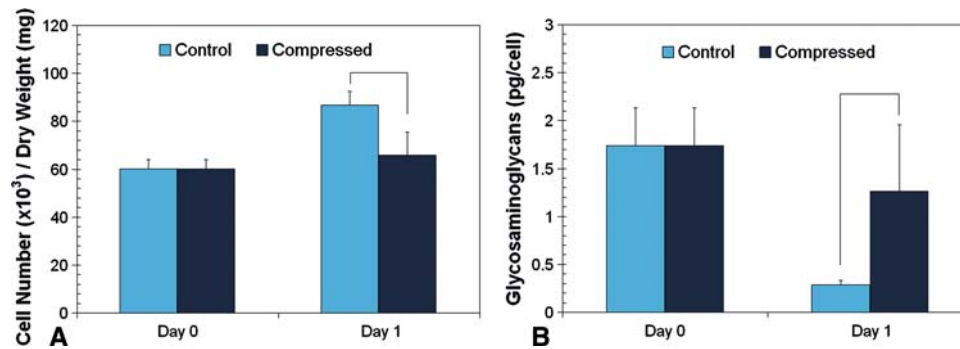


Fig. 6A–B Scaffold-induced compression modulated tendon cellularity and matrix composition. **A**) Cells proliferated in the unloaded control group and cell number was higher in the control compared to the compressed group after 24 hours of loading ($p = 0.0033$). **B**) Glycosaminoglycan content in the mesh was higher in the compressed group after 24 hours of loading ($p = 0.0342$).

matrix was evident in the control group by Day 14 (Fig. 5C). In general, collagen fibers remained perpendicular to the direction of loading after 24 hours, and this effect was maintained over 14 days with the mesh-collar scaffold complex (Fig. 5D). The total cell number in the tendons remained relatively constant in the compressed group, while we observed a higher ($p = 0.0033$) number of cells in the control tendons by Day 1 (Fig. 6A). Matrix glycosaminoglycan (GAG) content was greater ($p = 0.0342$) in the compressed tendon group after one day of loading (Fig. 6B), when compared to the unloaded control.

The mechanoactive mesh collar scaffold also promoted the expression of interface markers. After 24 hours of compression, gene expression of β brocartilage-related markers were upregulated in the loaded group when compared to uncompressed tendons (Fig. 7) with differences found in the expression of Type II collagen ($p = 0.0603$), aggrecan ($p = 3.11 \times 10^{-5}$), and TGF β 3 ($p = 3.66 \times 10^{-4}$).

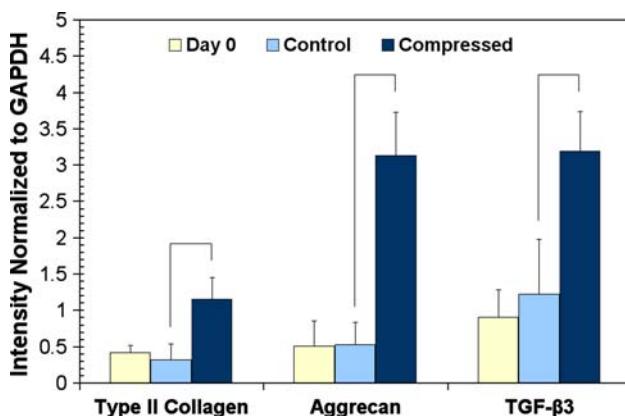


Fig. 7 Scaffold-induced compression of the tendon graft resulted in the up-regulation of β brocartilage markers, including type II collagen ($p = 0.0603$), aggrecan ($p = 3.11 \times 10^{-5}$), and TGF β 3 ($p = 3.66 \times 10^{-4}$) after 24 hours. Note the increase in all three β brocartilage interface-related markers in the tendon after scaffold-induced compression.

Discussion

Our long-term goal is to achieve biological fixation by engineering a functional and anatomical β brocartilage enthesis on biological and synthetic soft tissue grafts used in orthopaedic repair [39]. To this end, this study focused on the design and evaluation of two novel mechanoactive scaffold systems capable of applying mechanical loading, guided by the working hypothesis that, with the inherent contraction of PLGA nanofiber meshes, compression may be applied to tendon grafts, resulting in matrix remodeling and leading to β brocartilage formation. The first objective of this study was to characterize the contractile properties of an aligned nanofiber mesh versus the biphasic mesh+ collar scaffold complex; the second focused on the effect of scaffold-induced compression on β brocartilage development on a tendon graft. Specifically, we used the biphasic mesh+ collar scaffold to test the hypothesis that scaffold-induced compression of tendon grafts would result in matrix remodeling and the expression of β brocartilage markers.

We evaluated only tendon grafts with viable cells in this study. Allografts, which do not contain viable cells necessary for remodeling the tendon matrix, would need to be repopulated with β roblasts or stem cells delivered either from the scaffold or seeded in vitro before graft implantation. Mesenchymal stem cell-seeded Type I collagen sponges inserted into excised sheep patellar tendons and loaded using an ex vivo wrap-around system reportedly upregulated chondrogenic markers such as Sox9 and Fos [35]. A similar response by a devitalized tendon graft that has been repopulated with cells is anticipated following scaffold-mediated compressive loading. Moreover, the mesh-scaffold system is based on degradable polyhydroxyester polymers, thus it is expected the mechanoactive scaffold will be replaced by newly formed tissue after a functional β brocartilage interface has been formed on the graft. Future studies will focus on extending the

current study to longer time points, as well as evaluating the control and loaded groups. Proteoglycan content of the potential of coupling the mechanoactive scaffold with tendon matrix was also maintained in the loaded group ACL reconstruction grafts using physiologically relevant compared to the control, further indicating that scaffold-in vivo models. With the exception of proteoglycans, we induced compression influenced matrix maintenance and examined the effects of loading on Type II collagen and remodeling. These observations demonstrated the potential TGF- β 3 with gene expression and plan to extend these of this mesh+ collar scaffold system to provide continuous analyses to protein production. Additionally, other bio-mechanical stimulation and promote sustained tissue cartilage markers and regulatory factors may guide remodeling.

interface regeneration. Identifying these regulatory factors Scaffold-mediated compression also resulted in the is critical as it is anticipated that this novel scaffold system upregulation of bio-cartilage markers including Type II may be optimized to control the spatial and temporal distribution of relevant growth factors, thereby exercising (TGF- β 3). The bio-cartilage enthesis of tendons is largely biochemical stimulation to direct cellular differentiation comprised of types I and II collagen, as well as proteoglycans as well as promoting the transformation of the tendon glycans [4, 13, 32, 45]. Moreover, compressive loading of matrix into bio-cartilage through mechanical loading. Bio-cartilaginous regions of tendons enhances aggrecan

We observed that the mechanoactive scaffold was able to gene expression [13, 32] and increases the synthesis of to apply compressive loading to tendon grafts. Moreover, TGF- β 1 [52] and large proteoglycans. Compression of the scaffold-mediated compression promoted matrix remodeling in bio-cartilaginous regions of the deep flexor tendon also ing, maintained graft glycosaminoglycan content and promotes proteoglycan synthesis [43]. Our data are in interestingly, induced gene expression for bio-cartilage agreement with these published studies on the effects of interface-related markers, including Type II collagen, compressive loading, and demonstrate the feasibility of aggrecan, and TGF- β 3. These results demonstrate that implementing a degradable scaffold system for bio-cartilage-compressive loading can be incorporated into scaffold design interface formation on tendon grafts.

design and used to promote bio-cartilage formation on Contraction of PLGA meshes has been previously tendon grafts. reported in the literature [70], although the phenomenon

We described two scaffold-based loading systems. This has been discredited as a shortcoming rather than promoted first design involved using a nano-fiber mesh to directly as an advantageous attribute of the system. Currently, the load the tendon graft while the second design consisted of a mechanism underlying mesh contraction is not known. complex of the nano-fiber and microsphere-based graft [Zong et al. [70] reported electrospun nano-fiber mesh collar. The alignment of the nano-fiber mesh resulted in comprised of crystalline polyesters contracted less than anisotropic mesh contractile behavior, effectively translated amorphous polyester copolymers such as PLGA 75:25. It ing contractile force into compression, which was utilized was proposed that when nano-fiber meshes comprised of in this study to apply compressive loading to the tendon crystalline polymers are incubated at 37°C, the polymer grafts. In the first mechanoactive design, histological analysis revealed that nano-fiber-mediated contraction rapidly occurs, resulting in a lamellar structure that compression induced extensive remodeling of the tendon constrains the relaxation of the polymer chains and in turn ultrastructure, with the compressed graft exhibiting a prevents contraction [70]. The polyester copolymer utilized denser matrix with increased local cell density. This matrix in this study has a high D,L-lactide content (85%) and is modulation effect, however, diminished over time, with the non-crystalline, thus the above mechanism may explain the control and loaded groups nearly indistinguishable by Day high degree of contraction observed. Although not the 14. As mesh contraction stabilized after 24 hours, it is focus of the current study, fiber alignment-related scaffold likely the tendon graft no longer experienced mechanical anisotropy may be used to modulate mesh contraction, and stimulation in long-term cultures. Therefore, the short-term consequently, the magnitude and direction of compressive effect of mesh-induced compressive loading on graft loading on the graft may be controlled by customizing the matrix organization and the high magnitude of compression degree of fiber alignment. Future studies will focus on sion (approximately 30%) initiated the development of the elucidating the mechanism of mesh contraction as well as second mechanoactive scaffold system. Specifically, the exploring methods to control this process for mechanical nano-fiber mesh was combined with a degradable micro-

sphere-based graft collar system in order to achieve a lower We focused on the incorporation of mechanical loading compressive strain (15%). Under scaffold-induced compression, the remodeled tendon matrix with cells embedded the potential of using a mechanoactive scaffold system to in a dense matrix was maintained over time, with marked induce bio-cartilage formation on soft tissue grafts. This is differences in collagen matrix organization seen between advantageous for scaffold design as the mechanoactive

scaffold can be used to apply both physiological loading as well as desired ectopic loading in vitro and in vivo. For biological fixation, the mesh-collar system is intended to be applied clinically as a degradable graft collar, and will be used to initiate and direct regeneration of an anatomical fibrocartilage interface at the insertion of tendon-based ACL reconstruction grafts. In addition to providing a 3-D environment for matrix development and growth factors for guided cell differentiation, the innovative scaffold system described here can also apply physiologic mechanical stimulation crucial for directing cellular function and tissue remodeling. For utilization with viable autografts, we envision the graft would be inserted through the collars immediately before implantation, and compression of the graft and subsequent fibrocartilage formation would occur in vivo.

We described the design and evaluation of a mechanically active scaffold able to apply mechanical stimulation to tendon grafts. Scaffold-induced compression of the patellar tendon graft had a profound effect on matrix remodeling and led to the upregulation of fibrocartilage-related markers. These promising results demonstrate the clinical potential of the mechanoactive scaffold, as it is envisioned that the scaffold can be used to apply both biochemical and mechanical stimuli for the induction of metaplasia of the tendinous matrix, ultimately facilitating the formation of an anatomic fibrocartilage interface on these grafts. This approach offers promise as the functional transition between soft tissue and bone would be reestablished, with the potential to ensure long-term graft stability and improve clinical outcome through biological fixation.

Acknowledgments We thank Ms. Ciji Rich of the Biomaterials and Interface Tissue Engineering Laboratory at Columbia University for assistance in quantifying nanofiber mesh contraction, as well as Dr. X. Edward Guo of Columbia University for the use of the polarized light microscope for imaging collagen organization.

References

- Allum RL. BASK Instructional Lecture 1: graft selection in anterior cruciate ligament reconstruction. *Arthroscopy*. 2001;8:69D72.
- Arthroplasty and total joint replacement procedures: United States 1990 to 1997*. American Academy of Orthopaedic Surgeons; 2000.
- Benjamin M, Evans EJ, Copp L. The histology of tendon attachments to bone in man. *Anat*. 1986;149:89D100.
- Benjamin M, Ralphs JR. Fibrocartilage in tendons and ligaments: an adaptation to compressive load. *Anat*. 1998;193:481D494.
- Berg EE. Autograft bone-patella tendon-bone plug comminution with loss of ligament fixation and stability. *Arthroscopy*. 1996;12:232D235.
- Beynon B, Yu J, Huston D, Fleming B, Johnson R, Haugh L, Pope MH. A sagittal plane model of the knee and cruciate ligaments with application of a sensitivity analysis. *J Biomech Eng*. 1996;118:227D239.
- Beynon BD, Johnson RJ, Fleming BC, Peura GD, Renstrom PA, Nichols CE, Pope MH. The effect of functional knee bracing on the anterior cruciate ligament in the weightbearing and non-weightbearing knee. *Am J Sports Med*. 1997;25:353D359.
- Beynon BD, Meriam CM, Ryder SH, Fleming BC, Johnson RJ. The effect of screw insertion torque on tendons fixed with spiked washers. *Am J Sports Med*. 1998;26:536D539.
- Blickenstaff KR, Grana WA, Egle D. Analysis of a semitendinosus autograft in a rabbit model. *Am J Sports Med*. 1997;25:554D559.
- Brand J Jr, Weiler A, Caborn DN, Brown CH Jr, Johnson DL. Graft fixation in cruciate ligament reconstruction. *Am J Sports Med*. 2000;28:761D774.
- Burkart A, Imhoff AB, Roscher E. Foreign-body reaction to the bioabsorbable suretac device. *Arthroscopy*. 2000;16:91D95.
- Doshi J, Reneker DH. Electrospinning process and applications of electrospun fibers. *Electrostatics*. 1995;35:151D156.
- Evanko SP, Vogel KG. Proteoglycan synthesis in fetal tendon is differentially regulated by cyclic compression in vitro. *Arch Biochem Biophys*. 1993;307:153D164.
- Farndale RW, Sayers CA, Barrett AJ. A direct spectrophotometric microassay for sulfated glycosaminoglycans in cartilage cultures. *Connect Tissue Res*. 1982;9:247D248.
- Fleming B, Beynon B, Howe J, McLeod W, Pope M. Effect of tension and placement of a prosthetic anterior cruciate ligament on the anteroposterior laxity of the knee. *Orthop Res*. 1992;10:177D186.
- Fleming BC, Abate JA, Peura GD, Beynon BD. The relationship between graft tensioning and the anterior-posterior laxity in the anterior cruciate ligament reconstructed goat knee. *Orthop Res*. 2001;19:841D844.
- Friedman MJ, Sherman OH, Fox JM, Del Pizzo W, Snyder SJ, Ferkel RJ. Autogeneic anterior cruciate ligament (ACL) anterior reconstruction of the knee. A review. *Clin Orthop*. 1985;196:9D14.
- Gao J, Messner K, Ralphs JR, Benjamin M. An immunohistochemical study of enthesis development in the medial collateral ligament of the rat knee joint. *Anat Embryol (Berl)*. 1996;194:399D406.
- Goldblatt JP, Fitzsimmons SE, Balk E, Richmond JC. Reconstruction of the anterior cruciate ligament: meta-analysis of patellar tendon versus hamstring tendon autograft. *Arthroscopy*. 2005;21:791D803.
- Gotlin RS, Huie G. Anterior cruciate ligament injuries. Operative and rehabilitative options. *Phys Med Rehabil Clin N Am*. 2000;11:895D928.
- Gregor RJ, Abelew TA. Tendon force measurements and movement control: a review. *Med Sci Sports Exerc*. 1994;26:1359D1372.
- Grossman MG, ElAttrache NS, Shields CL, Glousman RE. Revision anterior cruciate ligament reconstruction: three- to nine-year follow-up. *Arthroscopy*. 2005;21:418D423.
- Hiss J, Hirshberg A, Dayan DF, Bubis JJ, Wolman M. Aging of wound healing in an experimental model in mice. *J Forensic Med Pathol*. 1988;9:310D312.
- Indelli PF, Dillingham MF, Fanton GS, Schurman DJ. Anterior cruciate ligament reconstruction using cryopreserved allografts. *Clin Orthop Relat Res*. 2004;420:268D275.
- Jackson DW, Grood ES, Arnoczky SP, Butler DL, Simon TM. Cruciate reconstruction using freeze dried anterior cruciate ligament allograft and a ligament augmentation device (LAD). An experimental study in a goat model. *Am J Sports Med*. 1987;15:528D538.
- Jiang J, Leong NL, Mung JC, Hidaka C, Lu HH. Interaction between zonal populations of articular chondrocytes suppresses

- chondrocyte mineralization and this process is mediated by PTHrP. *Osteoarthritis Cartil.* 2008;16:70D82.
27. Jiang J, Nicoll SB, Lu HH. Co-culture of osteoblasts and chondrocytes modulates cellular differentiation in vitro. *Biochem Biophys Res Commun.* 2005;338:762D770.
 28. Johnson DH. Should allografts be used for routine anterior cruciate ligament reconstructions? No, allografts should not be used for routine ACL reconstruction. *Arthroscopy.* 2003;19:424D425.
 29. Johnson RJ. The anterior cruciate: a dilemma in sports medicine. *Int J Sports Med.* 1982;3:71D79.
 30. Junqueira LC, Bignolas G, Brentani RR. Picrosirius staining plus polarization microscopy, a specific method for collagen detection in tissue sections. *Histochem J.* 1979;11:447D455.
 31. Junqueira LC, Montes GS, Sanchez EM. The influence of tissue section thickness on the study of collagen by the Picrosirius-polarization method. *Histochemistry.* 1982;74:153D156.
 32. Koob TJ, Clark PE, Hernandez DJ, Thurmond FA, Vogel KG. Compression loading in vitro regulates proteoglycan synthesis by tendon fibrocartilage. *Arch Biochem Biophys.* 1992;298:303D312.
 33. Kurosaka M, Yoshiya S, Andrich JT. A biomechanical comparison of different surgical techniques of graft fixation in anterior cruciate ligament reconstruction. *Am J Sports Med.* 1987;15:225D229.
 34. Kurzweil PR, Frogameni AD, Jackson DW. Tibial interference screw removal following anterior cruciate ligament reconstruction. *Arthroscopy.* 1995;11:289D291.
 35. Li KW, Lindsey DP, Wagner DR, Giori NJ, Schurman DJ, Goodman SB, Smith RL, Carter DR, Beaupre GS. Gene regulation ex vivo within a wrap-around tendon. *Tissue Eng.* 2006;12:2611D2618.
 36. Li WJ, Laurencin CT, Cateson EJ, Tuan RS, Ko FK. Electrospun nanofibrous structure: a novel scaffold for tissue engineering. *J Biomed Mater Res.* 2002;60:613D621.
 37. Loh JC, Fukuda Y, Tsuda E, Steadman RJ, Fu FH, Woo SL. Knee stability and graft function following anterior cruciate ligament reconstruction: Comparison between 11 o'clock and 10 o'clock femoral tunnel placement. *Arthroscopy.* 2003;19:297D304.
 38. Lu HH, El Amin SF, Scott KD, Laurencin CT. Three-dimensional, bioactive, biodegradable, polymer-bioactive glass composite scaffolds with improved mechanical properties support collagen synthesis, mineralization of human osteoblast-like cells in vitro. *J Biomed Mater Res.* 2003;64A:465D474.
 39. Lu HH, Jiang J. Interface tissue engineering and the formulation of multiple-tissue systems. *Adv Biochem Eng Biotechnol.* 2006;102:91D111.
 40. Lu HH, Tang A, Oh SC, Spalazzi JP, Dionisio K. Compositional effects on the formation of a calcium phosphate layer and the response of osteoblast-like cells on polymer-bioactive glass composites. *Biomaterials.* 2005;26:6323D6334.
 41. Malaviya P, Butler DL, Boivin GP, Smith FN, Barry FP, Murphy JM, Vogel KG. An in vivo model for load-modulated remodeling in the rabbit flexor tendon. *Orthop Res.* 2000;18:116D125.
 42. Markolf KL, Hame S, Hunter DM, Oakes DA, Zoric B, Gause P; Finerman GA. Effects of femoral tunnel placement on knee laxity and forces in an anterior cruciate ligament graft. *Orthop Res.* 2002;20:1016D1024.
 43. Matthews LS, Soffer SR. Pitfalls in the use of interference screws for anterior cruciate ligament reconstruction: brief report. *Arthroscopy.* 1989;5:225D226.
 44. Matyas JR, Anton MG, Shrive NG, Frank CB. Stress governs tissue phenotype at the femoral insertion of the rabbit MCL. *J Biomech.* 1995;28:147D157.
 45. Milz S, McNeilly C, Putz R, Ralphs JR, Benjamin M. Fibrocartilages in the extensor tendons of the interphalangeal joints of human toes. *Anat Rec.* 1998;252:264D270.
 46. Moffat KL, Sun WS, Pena PE, Chahine NO, Doty SB, Ateshian GA, Hung CT, Lu HH. Characterization of the mechanical properties and mineral distribution at the ligament-to-bone insertion site. *Proc Natl Acad Sci USA.* In Press.
 47. Nawata K, Minamizaki T, Yamashita Y, Teshima R. Development of the attachment zones in the rat anterior cruciate ligament: changes in the distributions of proliferating cells and fibrillar collagens during postnatal growth. *Orthop Res.* 2002;20:1339D1344.
 48. Perez-Castro AV, Vogel KG. In situ expression of collagen and proteoglycan genes during development of fibrocartilage in bovine deep flexor tendon. *Orthop Res.* 1999;17:139D148.
 49. Peterson RK, Shelton WR, Bomboy AL. Allograft versus autograft patellar tendon anterior cruciate ligament reconstruction: A 5-year follow-up. *Arthroscopy.* 2001;17:9D13.
 50. Poehling GG, Curl WW, Lee CA, Ginn TA, Rushing JT, Naughton MJ, Holden MB, Martin DF, Smith BP. Analysis of outcomes of anterior cruciate ligament repair with 5-year follow-up: allograft versus autograft. *Arthroscopy.* 2005;21:774D785.
 51. Rich L, Whittaker P. Collagen and picrosirius red staining: a polarized light assessment of fibrillar hue and spatial distribution. *Braz J Morphol Sci.* 2005;22:97D104.
 52. Robbins JR, Evanko SP, Vogel KG. Mechanical loading and TGF-beta regulate proteoglycan synthesis in tendon. *Biochem Biophys.* 1997;342:203D211.
 53. Robertson DB, Daniel DM, Biden E. Soft tissue fixation to bone. *Am J Sports Med.* 1986;14:398D403.
 54. Rodeo SA, Arnoczky SP, Torzilli PA, Hidaka C, Warren RF. Tendon-healing in a bone tunnel. A biomechanical and histological study in the dog. *J Bone Joint Surg Am.* 1993;75:1795D1803.
 55. Rodeo SA, Suzuki K, Deng XH, Wozney J, Warren RF. Use of recombinant human bone morphogenetic protein-2 to enhance tendon healing in a bone tunnel. *Am J Sports Med.* 1999;27:476D488.
 56. Shellock FG, Mink JH, Curtin S, Friedman MJ. MR imaging and metallic implants for anterior cruciate ligament reconstruction: assessment of ferromagnetism and artifact. *Magn Reson Imaging.* 1992;2:225D228.
 57. Shelton WR, Papendick L, Dukes AD. Autograft versus allograft anterior cruciate ligament reconstruction. *Arthroscopy.* 1997;13:446D449.
 58. Sherman OH, Banffy MB. Anterior cruciate ligament reconstruction: which graft is best? *Arthroscopy.* 2004;20:974D980.
 59. Spalazzi JP, Dagher E, Doty SB, Guo XE, Rodeo SA, Lu HH. In vivo evaluation of a multi-phased scaffold designed for orthopaedic interface tissue engineering, soft tissue-to-bone integration. *J Biomed Mater Res.* 2008; www.interscience.wiley.com DOI: 10.1002/jbm.a.32073
 60. Spalazzi JP, Doty SB, Moffat KL, Levine WN, Lu HH. Development of Controlled Matrix Heterogeneity on a Triphasic Scaffold for Orthopedic Interface Tissue Engineering. *Tissue Eng.* 2006;12:3497D3508.
 61. Spalazzi JP, Gallina J, Fung-Kee-Fung SD, Konofagou EE, Lu HH. Elastographic imaging of strain distribution in the anterior cruciate ligament and at the ligament-bone insertion. *Orthop Res.* 2006;24:2001D2010.
 62. Vanderploeg EJ, Imler SM, Brodtkin KR, Garcia AJ, Levenston ME. Oscillatory tension differentially modulates matrix metabolism and cytoskeletal organization in chondrocytes and fibrochondrocytes. *J Biomech.* 2004;37:1941D1952.
 63. Vogel KG. The effect of compressive loading on proteoglycan turnover in cultured fetal tendon. *Connect Tissue Res.* 1996;34:227D237.
 64. Wagner M, Kaab MJ, Schallock J, Haas NP, Weiler A. Hamstring tendon versus patellar tendon anterior cruciate ligament reconstruction using biodegradable interference fixation: a prospective matched-group analysis. *Am J Sports Med.* 2005;33:1327D1336.

65. Wang IN, Mitroo S, Chen FH, Lu HH, Doty SB. Age-dependent changes in matrix composition and organization at the ligament-to-bone insertion *J Orthop Res.* 2006;24:1745-1755.
66. Weiler A, Peine R, Pashmineh-Azar A, Abel C, Sudkamp NP, Hoffmann RF. Tendon healing in a bone tunnel. Part I: Biomechanical results after biodegradable interference fixation in a model of anterior cruciate ligament reconstruction in sheep. *Arthroscopy.* 2002;18:113-123.
67. Woo SL, Buckwalter JA. AAOS/NIH/ORS workshop. Injury and repair of the musculoskeletal soft tissues. Savannah, Georgia, June 18-20, 1987. *Orthop Res.* 1988;6:907-931.
68. Woo SL, Gomez MA, Seguchi Y, Endo CM, Akeson WH. Measurement of mechanical properties of ligament substance from a bone-ligament-bone preparation *Orthop Res.* 1983;1:22-29.
69. Yang F, Murugan R, Wang S, Ramakrishna S. Electrospinning of nano/micro scale poly(L-lactic acid) aligned fibers and their potential in neural tissue engineering *Biomaterials.* 2005;26:2603-2610.
70. Zong X, Ran S, Kim KS, Fang D, Hsiao BS, Chu B. Structure and Morphology Changes during in vitro Degradation of Electrospun Poly(glycolide-co-lactide) Nanofiber Membranes *Biomacromolecules.* 2003;4:416-423.